Current Applied Science and Technology Vol. 22 No. 6 (November-December 2022)

Research article

Oxidation Behavior of Nanostructure Sputtered Titanium Nitride Thin Films

Adisorn Buranawong[1,2] and Nirun Witit-Anun[1,2] *

[1]*Department of Physics, Faculty of Science, Burapha University, Chonburi, Thailand*
[2]*Thailand Center of Excellence in Physics, Ministry of Higher Education, Science, Research and Innovation, Bangkok, Thailand*

Received: 23 August 2021, Revised: 13 February 2022, Accepted: 17 April 2022

DOI: 10.55003/cast.2022.06.22.015

Keywords

thermal oxidation;

TiN;

magnetron sputtering

Abstract

The oxidation behavior of reactive DC magnetron sputtered TiN thin films was investigated under annealing temperature ranging from 400 to 700ºC in the ambient atmosphere using X-ray diffraction, energy dispersive X-ray spectroscopy, and field-emission scanning electron microscopy techniques. The oxidation rate and oxidation activation energy of the films were also calculated from parabolic and Arrhenius relations. The as-deposited film had a polycrystalline TiN structure. After annealing at 450ºC, the TiO_2 rutile structure was found in the XRD spectra and the relative integrated intensity of the oxide phase increased gradually with temperature. The EDS analysis gave confirmation of XRD patterns, showing the expected increase in O content. Grain growth resulting from grain coalescence occurred through the annealing temperatures. The cross-sectional analysis showed that a very thin dense oxide overlayer was present at 400°C and the oxide thickness increased gradually with temperature. Moreover, the films were fully oxidized into a porous structure after 650ºC. The results revealed that the films showed an oxidation rate from 400°C and the oxidation activation energy of films was 156.56 kJ/mol.

1. Introduction

Over many decades, oxides and nitrides compound thin films have long been of interest due to their outstanding physical and chemical properties such as good chemical stability, high hardness, and good magnetic properties [1, 2]. Owing to these properties, transition metal nitrides have been used in a wide range of technological applications, for example, as wear and corrosion resistant coatings, and hard coatings [3-5]. Among the transition metal nitrides, titanium nitride (TiN) has often been used as a hard coating to achieve on lower friction, more wear resistance, better oxidation resistance,

*Corresponding author: Tel.: (+66) 38103084 Fax: (+66) 38103084
E-mail: nirun@buu.ac.th

and increased tool performance and lifetime in machining tools and cutting tools [6, 7]. In its hard coating industrial applications, TiN thin film was directly subjected to extreme oxidizing conditions resulting in its mechanical and tribological characteristics at high temperature deteriorated, and thus it is very important to investigate the oxidation behavior of TiN thin film at elevated temperatures.

A number of studies of the oxidation behavior of TiN thin films using various characterization technique were previously carried out, for example, thermo gravimetric analysis (TGA) [8], X-ray photoelectron spectroscopy (XPS) [9], Rutherford back scattering (RBS) [10], and auger electron spectroscopy (AES) [11]. Due to limitations, these techniques could not be used to fully characterize the oxide morphology. However, field emission scanning electron microscope (FE-SEM) analysis has proved to be a useful tool because the changes in surface morphology and cross-sectional morphology during oxidation can be simultaneously observed. Moreover, the oxidation kinetics and activation energy associated with the formation of the oxide layer on a TiN film surface when exposed to an oxidizing environment at different temperatures, which brought about a clearer understanding of the film's oxidation behavior [12].

The oxidation behavior of TiN thin film at elevated temperatures has been reported by many researchers [10-16]. It was found that the range of oxidizing temperature from 550°C to a high temperature (1000°C) with an increased step of 100°C for each sample had been well researched, but the temperatures ranging across the oxidation temperature (500°C) with smaller incremental increases in oxidizing temperature, that is, steps of less than 100°C (50°C), has been less dealt with. Moreover, it is believed that the latter lower temperature range with smaller incremental increases was needed for a deeper understanding of oxidation behavior in the transition region. The aim of the present study was to investigate the thermal oxidation behavior of DC magnetron sputtered nanostructure TiN thin film anneal at elevated temperatures ranging from 400-700°C for 2 h with short step temperature increase of 50°C under atmosphere. The phase evolution, morphological change, cross-sectional morphologies, and activation energy were also studied and discussed in details.

2. Materials and Methods

2.1 Deposition of TiN thin films

A homemade closed field unbalanced reactive DC magnetron sputtering system was used to deposit nanostructured TiN thin films on silicon (100) substrates. The deposition system is a cylindrical chamber equipped with a single unbalanced magnetron. A vertical mount of circular flat magnetrons 2" in diameter and 3 mm thickness was connected to the DC power supply. Ti (99.97%) purity was used as the sputtering target for growing the coating. For the pumping system, a diffusion pump was used, and it was assisted by a rotary pump. Before loading into the deposition chamber, the substrates were ultrasonically cleaned in acetone and ethanol for 10 min each, then blown dried before transferring to the deposition process.

The base pressure was evacuated to 5.0 x 10^{-5} mbar. Before the coating was obtained, a pre-sputtered process was performed by bombardment of Ar ions to remove surface contaminates. The working pressure during sputtering of 5.0 × 10^{-3} mbar was maintained throughout the deposition process. The Ar (99.999%) and N (99.999%) gases were used as the working gases for sputtering and reactive gas to form nitrides, respectively, with a fixed flow rate at 20 to 3 sccm. The current applied to the Ti target was 700 mA. The film deposition was carried out for 60 min. The entire deposition process was carried out without any external heating and the substrates were installed on a substrate holder which floated. The distance of Ti target to a substrate was 10 cm.

2.2 Annealing of TiN thin films

In order to anneal the film in the ambient atmosphere after the deposition process, the deposited TiN on the substrate was loaded into a tube furnace (CARBOLITE : CWF 13/5) using a thermocouple to monitor the temperature during thermal oxidation. Annealing took place in the furnace chamber in which the samples were placed in small Al_2O_3 crucibles. The annealing temperature ranged from 400 to 700ºC with stepped increase of 50ºC for each sample. The exposure time was held at 2 h throughout this work. The deposited samples were first naturally cooled down to room temperature in the furnace before moving out for the next analyses.

2.3 Thin films characterizations

The changes in the crystal structure and phase compositions of the as-deposited thin films and formed oxide layer during thermal oxidation at different temperatures were investigated by X-ray diffraction (XRD) (Bruker : Model D8) equipped with X-ray tubes using Cu Kα radiation ($\lambda_{Cu\ K\alpha}$ = 0.154 nm) in the θ/2θ mode. Measurement was operated at U = 40 kV and I = 40 mA with a grazing incident angle of 5º. The XRD pattern was recorded over the 2θ ranging from 20 to 80 degrees, and the collection interval and scanning rate were 0.02º and 3º/min for each sample. The chemical composition of the as-deposited and oxidized thin films was analyzed by energy dispersive X-ray spectroscopy (EDS). The surface morphologies, microstructures, and cross-sectional morphologies during thermal oxidation in the ambient atmosphere were observed using a Hitachi S-4700 field-emission scanning electron microscope (FE-SEM), which operated at an acceleration voltage of 50 kV.

2.4 Oxidation behavior of thin film

Oxidation behavior has been discussed in terms of the oxidation rate constant ($k_{p(T)}$) and oxidation activation energy (E_a) at a given temperature following a parabolic relation [17]. The oxidation rate constant, which is defined as the growth of an oxide film by thermal oxidation, is usually discussed in terms of Wagner's parabolic oxidation relation, as shown in equation 1.

$$d = 2\sqrt{k_p(t) \times t} \tag{1}$$

Where d is the thickness of the oxide layer from cross-sectional analysis and t is the thermal oxidation time of exposure at different temperatures (2 h).

The oxidation activation energy, which is the minimum amount of energy that must be provided for oxide compounds to undergo thermal oxidation, is calculated by plotting the curve from the Arrhenius-type equation using the $k_{p(T)}$ from equation 2.

$$k_p(T) = k_{p0} \exp\left(\frac{-E_a}{RT}\right) \tag{2}$$

Where k_{p0} is the pre-exponential factor, E_a is oxidation activation energy, R is gas constant and T is the absolute temperature. Hence, E_a was obtained from the slope of the curve.

3. Results and Discussion

3.1 The crystal structure of TiN thin films

The crystal structure and phase of as-deposited film and film after oxidation in the air for 2 h at various temperatures as identified by X-ray diffraction analyses were shown in Figure 1. It was revealed that the diffraction angles of as-deposited thin films were 36.68º, 42.34º, and 61.64º. The diffraction peaks were in good agreement with the JCPDS standard for TiN (JCPDS no.87-0633) as (111), (200), and (220) planes. The X-ray pattern of as-deposited films showed strong preferred orientations in the TiN (100) plane. At annealing temperature of 400 ºC, the TiN (200) was the preferred orientation. The additional of the 2θ peak at 35.72º, which was in good agreement with the JCPDS standard (JCPDS no.89-4920) for the tetragonal TiO_2 rutile structure of (101) plane mixed with all TiN (111), (200), and (220) planes, was identified at oxidation temperature of 450ºC.

The X-ray intensity was increased for both of TiO_2 and TiN structures; however, a strong preferred orientation was exhibited for the TiN (111) plane at 500 ºC. As the oxidation temperature increased to 550 ºC, a significant enhancement of crystallinity with strong preferred orientations along TiO_2 (101) planes was seen, whereas the diffraction patterns of TiN (200) and (311) planes were identified. The integrated diffraction pattern at 2θ of 36.2º, 41.4º, 54.6º, 56.2º 63.1º, and 70.1º which represented only the TiO_2 rutile structure (101), (111), (211), (220), (002), and (112) planes with strong intensity peak (101) planes were exhibited at 600ºC. Further increase in oxidation temperature to 650ºC resulted in no change for all peaks. As the oxidation temperature reached 700ºC, there was decreased intensity at the (100) plane, whereas the TiO_2 peak (110) plane was identified at the 27.5º diffraction angle, respectively. Furthermore, the crystallite size of TiO_2 peak, which was calculates from Scherrer's equation, was obtained from the XRD pattern. There was an enhancement of crystallite size from 7.1 to 28.7 nm as the oxidation temperature increased from 450-700ºC.

It can be concluded that the as-deposited TiN thin film started to transform into the rutile-TiO_2 tetragonal structure at an oxidation temperature of 450°C and then completely changed into TiO_2 (Figure 1) above this value. The results also implied that the film oxidized at 450°C. The peaks of TiN before the study of the oxidation behavior included the (111), (200), and (220) planes. At 450ºC, the TiN and TiO_2 phase mixture was investigated. Traces of rutile type tetragonal structure phase was clearly identified at this temperature. However, under the conditions of thermal oxidation ranging between 400-550ºC, the mixed structure of TiN and oxide TiO_2 peak structure was found. The intensity of TiO_2 rapidly increased and that of TiN decreased, indicating a small fraction of the films had oxidized. Moreover, the transition region of crystal structure transformation was noticed in this work. When temperature ranged from 600-700ºC, the TiO_2 peaks indicated that the film had totally oxidized. This result was attributed to the oxygen from the annealing atmosphere reacting with the TiN thin films which resulted in forming the TiO_2 by oxidation mechanism [13]. Furthermore, the transformation of the cubic TiN into the rutile TiO_2 phase observed in this work was consistent with the findings of previous literatures [12-15]. Moreover, the increase of TiO_2 crystallite size was due to thermal induction of the film structure. Thus, the results confirmed the oxidation behavior during thermal oxidation process.

3.2 The chemical composition of TiN thin film

The chemical composition of TiN thin film samples before and after thermal oxidation was further analyzed by the EDS technique. Figure 2 illustrates the investigations of chemical composition as a function of thermal oxidation temperature under air atmosphere. The as-deposited TiN thin film

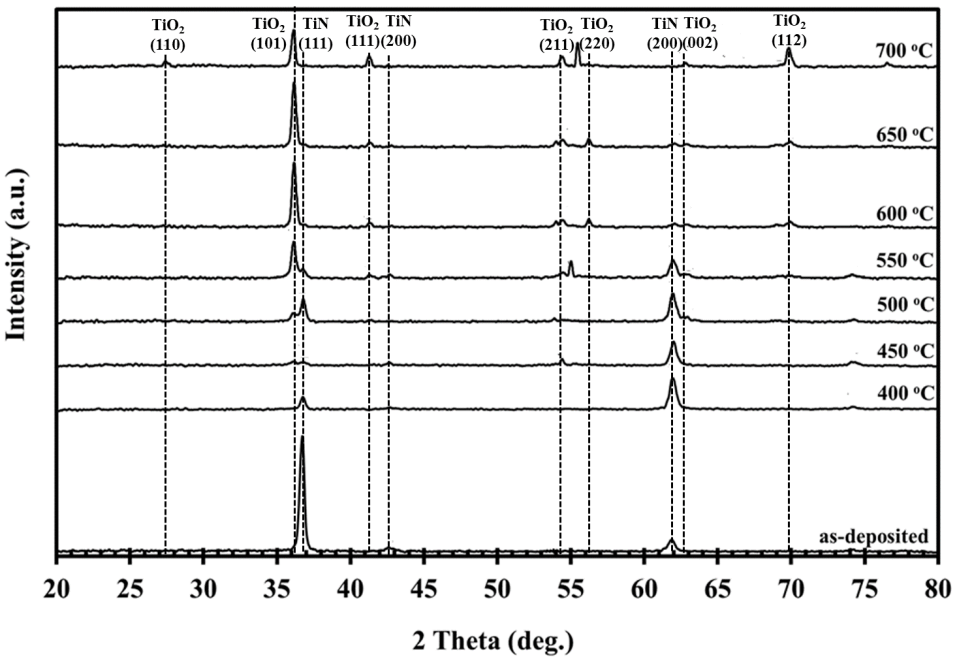

Figure 1. The XRD pattern of the TiN thin films before and after annealing in the air for 2 h

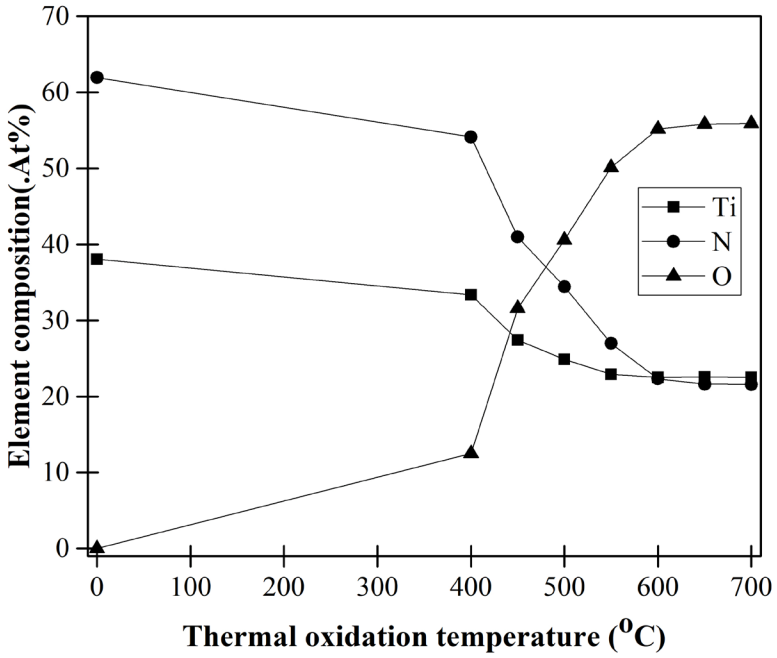

Figure 2. The element compositions of the TiN thin films before and after annealing in the air for 2 h at a various temperatures ranging from 400 to 700ºC

contained Ti and N compositions of 38.06 and 61.94 (at.%), respectively. The low oxygen (O) content of 12.52 (at.%) with Ti (33.36 at.%) and N (54.12 at.%), respectively, were seen at the oxidation temperature of 400ºC. At 450ºC, a significant increase by almost three times of O content to 31.60 at% occurred, whereas there were reductions in the Ti content to 27.41 (at.%) and N to 40.98 (at%). There was a slightly increase in O composition from 40.60 to 50.12 (at.%) but decreases in Ti and N content from 24.89 to 22.90 (at.%) and 34.43 to 26.98 (.at%), respectively, were exhibited as the thermal oxidation temperature moved from 500-600ºC. At thermal oxidation temperature ranging from 600-700, Ti, N, and O compositions remained constant in the ranges of 22.55 to 22.50 (at.%), 22.32 to 21.58 (at.%) and 55.17 to 55.92 (at.%), respectively.

The chemical composition analysis results were in good agreement with the results of the crystal structure characterization, further suggesting that the as-deposited samples without annealing treatment exhibited a TiN structure whereas the samples subjected to thermal oxidation from 400-700ºC had a changing structure with phase segregation due to the heating process. The increase of O content during the thermal oxidation between 400-600ºC occurs due to the inward diffusion of O from the atmosphere diffusing directly onto the film replacing N in the TiN structure. The addition of O and the reduction of N by the oxidation mechanism with increase temperature [14, 16] can be identified from the EDX results. In addition, the constancy of element compositions of Ti, N, and O at high thermal oxidation temperature (600-700ºC) is due to the saturation of the O atoms that diffuse into the intercolumnar spacing of the films [11]. Another explanation is that it is possible that O content might come from the oxygen trapped in the grain boundaries of TiN. Based on the present experiment, the EDX results clearly confirm the XRD diffraction patterns in terms of the crystal structure transformation to oxide phase through the oxidation process and the oxidation behavior was also observed.

3.3 Surface and cross-sectional morphologies of TiN thin film

The surface morphology changes of TiN thin films before and after the thermal oxidation at 400-700ºC in steps of 50ºC in the air for 2 h are illustrated in the FE-SEM images in Figure 3. A tapered structure of the same size and density of pattern was spread across the surface of non-oxidized films (Figure 3a). Similar surface features with slightly increased grain sizes were observed for film annealed at 400ºC (Figure 3b). At 450ºC, significant changes to the grains had occurred. The grains had become facet-like structures with small voids between the grain boundaries in some areas of the film surface, as shown in Figure 3c. When the thermal oxidation temperature was further increased to 500ºC, no change of grains was obtained (Figure 3d). A similar grain type but with more void on film surface appeared at 550ºC, as illustrated in Figure 3e. The grain size gradually grew and there was a more open surface between grain boundaries at 600ºC, as revealed in Figure 3f. The growth of facet grains and the presence of big voids became evident on the surface at 650ºC, as shown in Figure 3g. The larger grain boundaries and different sizes of facet-grain scattered across the surface can be clearly seen after the samples were subjected to 700ºC (Figure 3h).

It is interesting to note that when the thermal oxidation temperature was increased, the TiN surface morphology evolved from as-deposited nano tapered compacted structures to a mixture of TiO_2 irregular faceted grains at the highest temperature of 700ºC. The grain sizes of the TiO_2 structure obviously had more enlarged voids and open surfaces between grain boundaries as oxidation temperature increased. This was probably due to the additional thermal energy provided at higher temperatures and then increased the mobility of deposited atoms resulting in a grain coalescence effect [17]. Moreover, another reason was the grain growth mechanism involving the transfer of atoms at grain boundaries from one to another with increase in annealing temperature [18]. Therefore, the surface morphologies of TiO_2 became dominant at temperatures above 450ºC.

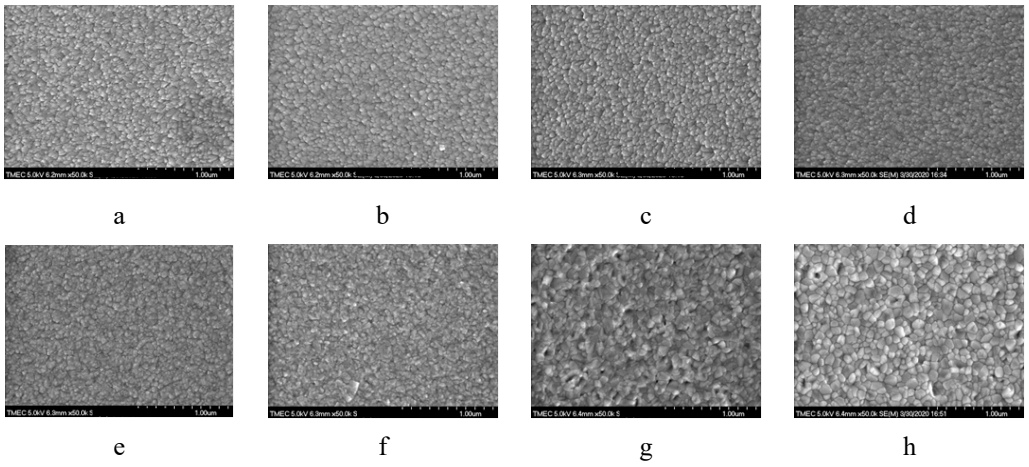

Figure 3. Plane view surface morphology micrographs of (a) as-deposited TiN thin film and the film oxidized in air, (b) 400ºC, (c) 450ºC, (d) 500ºC, (e) 550ºC, (f) 600ºC, (g) 650ºC, and (h) 700ºC for 2 h

The result of the present work corresponded to that of other researchers who also found that grain aggregation was a function of oxidation temperature [12, 17].

The oxidation behavior of the films investigated by XRD and EDX techniques was verified by FE-SEM. Figure 4 illustrates the cross-sectional micrographs of the as-deposited TiN thin film and after annealing at 400-700ºC. The film and oxide thickness are also listed in Table 1. A dense columnar pattern that contained long columnar grains with clear grain boundaries throughout the film thickness was observed for the un-oxidized film (Figure 4a). A very thin and dense protective oxide layer was formed on the film surface whereas the bottom TiN layer was retained the columnar structure at 400ºC (Figure 4b). At an annealing temperature of 450ºC, a slightly increase in thickness and grain growth of TiO_2 overlayer was observed, and meanwhile, more voids between grain boundaries at the bottom of the film were found (Figure 4c).

The grain aggregation, porous structure, and significant increase in the oxide layer accompanying with the appearance of disordered long columnar grain structure and clear grain boundaries of the TiN layer clearly appeaedr at the annealing temperature of 500ºC, as shown in Figure 4d. At an annealing temperature of 550ºC, the oxide layer showed a more porous structure with the larger grain size in almost all of the top half of the film, and also more of the columnar pattern occurred. The TiO_2 layer had an obvious grain size agglomeration with large amounts of void structures whereas the dense columnar structure of TiN under the top oxide layer can be observed from the film oxidized at 600ºC (Figure 4f). After annealing the film at 650ºC, the underlying TiN columnar structure disappeared and was replaced with short columnar grain, indicating that the film was fully oxidized (Figure 4g). The porous structure and grain developed along the oxide thickness in the film at the highest annealing temperature of 700ºC (Figure 4h). Not only the oxide layer was enhanced from 20 to 1372 nm but there was also an induction of the overall thickness of the bottom layer (TiN) combined with the top oxide layer (TiO_2) from 815 to 1372 nm, respectively, with increase of annealing temperature (Table 1) because of the O from the atmosphere reacted more with the TiN film. This oxide thickness enhancement resultrd in the total thickness increase with increased annealing temperature [11, 13].

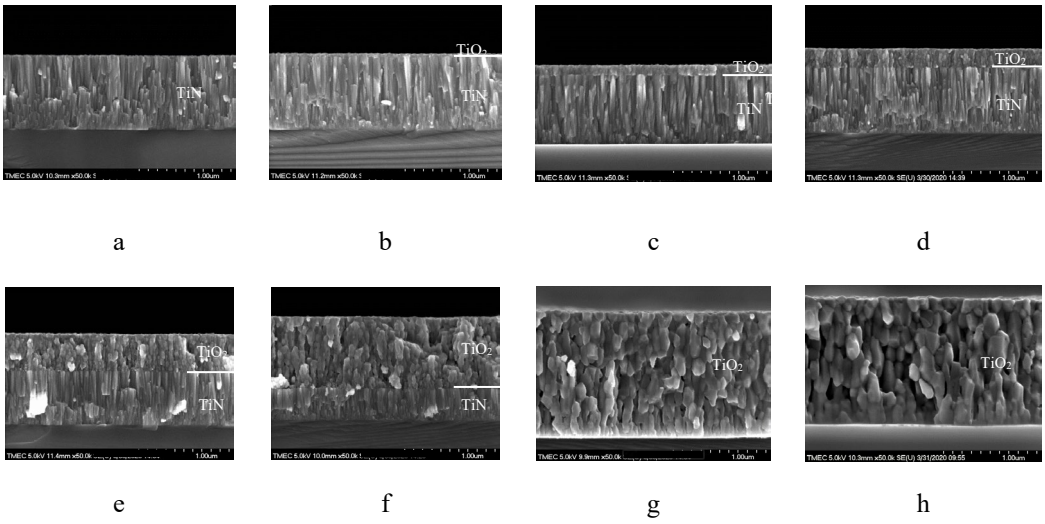

Figure 4. Cross sectional micrographs of (a) as-deposited TiN thin film and the film oxidized in air, (b) 400ºC, (c) 450ºC, (d) 500ºC, (e) 550ºC, (f) 600ºC ,(g) 650ºC, and (h) 700ºC for 2 h

Table 1. The film thickness, oxide thickness and oxidation rate of TiN thin films before and after annealing at different temperatures

Annealing Temperature (ºC)	Film Thickness (nm)	Oxide Thickness (nm)	Oxidation Rate (cm^2/s)
As - deposited	804	-	-
400	815	20	1.89×10^{-16}
450	834	100	3.66×10^{-15}
500	901	230	1.38×10^{-14}
550	1002	420	5.90×10^{-14}
600	1136	780	2.13×10^{-13}
650	1372	1372	6.54×10^{-13}
700	1372	1372	6.54×10^{-13}

The transformation of the dense columnar structure of as-deposited TiN into the porous structure with short columnar grains was clearly observed with increased oxidation temperature and the film was completely transformed to oxide above 600ºC. This result can be explained by the growth of oxide along the film thickness being controlled by inward diffusion of O from air replacing N to form TiO_2 with N migrating into the atmosphere during oxidation process [11, 13]. Another explanation is that a columnar structure which has been deposited by the PVD technique is typical achieved [19, 20], and therefore oxygen diffuses easily along the grain boundary and further reacts with the nitride to form an oxide [11-14, 19]. The oxide layer from the FE-SEM result was in a good agreement with the TiO_2 rutile structure of the film annealed at 400-700ºC obtained from XRD patterns. It was observed that the cross-sectional analysis by FE-SEM was a very useful technique to investigate the thermal oxidation behavior as it gave a direct measurement of the oxide layer.

3.4 Oxidation behavior of TiN thin film

The oxidation rates at different thermal oxidation temperatures of TiN thin films are listed in Table 1. The oxide layer from cross-sectional FE-SEM was also taken to calculate the oxidation rate. It can be seen that the films had oxidation rates in the temperature range from 400ºC to 700ºC. The enhancement of oxidation rate from 1.89×10^{-16} cm^2/s to 6.52×10^{-16} cm^2/s was found throughout the oxidation temperature range. In addition, the Arrhenius plot ln $k_{p(T)}$ as a function of thermal oxidation temperature for TiN thin film is shown in Figure 5. The oxidation activation energy which is obtained from the slope of linear regression was calculated to be 163.37 kJ/mol.

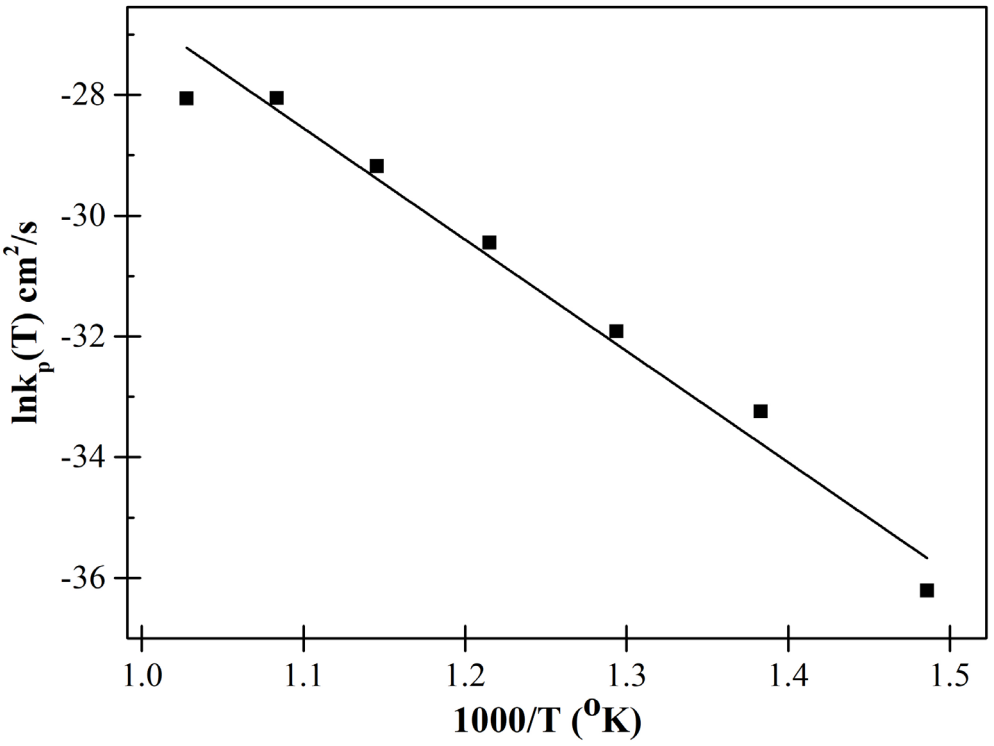

Figure 5. Arrhenius plot of TiN thin films oxidized at various annealing temperatures in air

It is revealed that the oxide layer growth followed a parabolic growth law, implying that the oxidation behavior that took place was induced by the annealing process. The oxidation activation energy of this work was different from those values found in previous study, which were 110±10 kJ/mol [12], 113.85±13, 118.93±16 kJ/mol [19] and 166±3 kJ/mol [21]. This deviation may be related to the as-deposited microstructures from various deposition conditions strongly influencing the rate and activation energy of oxidation that are mentioned in the other works [12, 17, 21]. Additionally, different oxidation conditions also affected the oxidation behavior of the films.

4. Conclusions

The thermal oxidation behavior of reactive DC magnetron sputtered TiN thin films was investigated over an oxidation temperature range of 400°C-700°C for exposure time of 2 h at an ambient atmosphere using X-ray diffraction, energy-dispersive X-ray spectroscopy, and field- emission scanning electron microscopy. The annealing process led to the formation of TiO_2 rutile structure from 450°C, which appeared in the XRD spectra and the X-ray intensity evolved with thermal oxidation temperature, which was due to oxygen from the atmosphere reacting with the TiN thin film. The EDS analysis confirmed the XRD patterns which coincided with an increase in O content from 12.52 to 55.92 (at.%) with increased oxidation temperature. Grain growth and increased void between grain boundaries due to aggregation effect were identified from surface morphologies using FE-SEM. The cross-sectional analysis suggested that a dense columnar structure existed in the as-deposited TiN whereas the porous structure was found during oxidation and it resulted from an inward diffusion mechanism. The oxide overlayer and film thickness increased significantly with oxidation temperature. The FE-SEM results were in good agreement with the XRD and EDS observations. The oxidation rate and oxidation activation energy obtained from the analysis of the parabolic and Arrhenius relations ranged from 1.89×10^{-16} cm^2/s to 6.54×10^{-13} cm^2/s, respectively.

5. Acknowledgements

This work was supported by Burapha University Research and Development Fund.

References

[1] Wushuer, M., Xiaerding, F., Mamat, M., Xu, Ma., Mijiti, A. and Aihaiti, L., 2020. Influence of Mn doping on structural, optical, and magnetic properties of $BiFeO_3$ films fabricated by the sol-gel method. *Science Asia*, 46, 330-335.

[2] Sun, N., Xu, J., Zhou, D., Zhao, P., Li, S., Wang, J., Chu, S. and Ali, F., 2018. DC reactively sputtered TiN_x thin films for capacitor electrodes. *Journal of Materials Science: Materials in Electronics*, 29, 10170-10176.

[3] Wu, W.Y., Chan, M.Y., Hsu, Y.H., Chen, G.Z. Liao, S.C. Lee, C.H. and Lui, P.W., 2019. Bio application of TiN thin films deposited using high power impulse magnetron sputtering. *Surface and Coatings Technology*, 362, 167-175.

[4] Yi, P., Zhu, L., Dong, C. and Xiao, K., 2019 Corrosion and interfacial contact resistance of 316L stainless steel coated with magnetron sputtered ZrN and TiN in the simulated cathodic environment of a proton-exchange membrane fuel cell. *Surface and Coatings Technology*, 198-202.

[5] Yang, J., Peng, M., Liao, J., Yang, Y. and Liu, N., 2017. Effect of N_2 gas injection parameters on structure and properties of TiN thin films prepared by reactive gas pulse sputtering. *Surface and Coatings Technology*, 311, 391-397.

[6] Bejaxhin, A.B.H. and Paulraj, G., 2019. Experimental investigation of vibration intensities of CNC machining centre by microphone signals with the effect of TiN/epoxy coated tool holder. *Journal of Mechanical Science and Technology*, 33, 1321-1331.

[7] Kıvak, T., Sarıkay, M., Yıldırım, Ç.V. and Şirin, Ş., 2020. Study on turning performance of PVD TiN coated Al_2O_3+TiCN ceramic tool under cutting fluid reinforced by nano-sized solid particles. *Journal of Manufacturing Processes*, 56, 522-539.

[8] Ichimura, H. and Kawana, A., 1993. High-temperature oxidation of ion-plated TiN and TiAlN films. *Journal of Materials Research*, 8, 1093-1100.
[9] Avasarala, B. and Haldar, P., 2010. Electrochemical oxidation behavior of titanium nitride based electrocatalysts under PEM fuel cell conditions. *Electrochimica Acta*, 55, 9024-9034.
[10] Montero, I., Jiménez, C. and Perrière, J., 1991. Surface oxidation of TiN_x films. *Surface Science*, 251-252, 1038-1043.
[11] Logothetidis, S., Meletis, E.I., Stergioudis, G. and Adjaottor, A.A., 1999. Room temperature oxidation behavior of TiN thin films. *Thin Solid Films*, 388, 304-313.
[12] Chen, H.-Y. and Lu, F.-H. 2005. Oxidation behavior of titanium nitride films. *Journal of Vacuum Science and Technology A*, 23, 1006-1009.
[13] Aliaj, F., Syla, N., Oettel, H. and Dilo, T., 2016. Thermal treatment in air of direct current (DC) magnetron sputtered TiN coatings. *Scientific Research and Essays*, 11, 230-238.
[14] Chim, Y.C., Ding, X.Z., Zeng, X.T. and Zhang, S., 2009. Oxidation resistance of TiN, CrN, TiAlN and CrAlN coatings deposited by lateral rotating cathode arc. *Thin Solid Films*, 517, 4845-4849.
[15] Fateh, N., Fontalvo, G.A., Gassner, G. and Mitterer, C., 2009. Influence of high-temperature oxide formation on the tribological behaviour of TiN and VN coatings. *Wear*, 262, 1152-1158.
[16] Glaser, A., Surnev, S., Netzer, F.P., Fateh, N., Fontalvo, G.A. and Mitterer, C., 2007. Oxidation of vanadium nitride and titanium nitride coatings. *Surface Science*, 601, 1153-1159.
[17] Qi, Z.B., Liu, B., Wu, Z.T., Zhu, F.P., Wang, Z.C. and Wu, C.H., 2013. A comparative study of the oxidation behavior of Cr_2N and CrN coatings. *Thin Solid Films*, 544, 515-520.
[18] Jafari, A., Ghoranneviss, Z., Elahi, A.S., Ghoranneviss, M., Yazdi, N.F. and Rezaei, A., 2014. Effect of annealing on TiN thin films growth by DC magnetron sputtering. *Advance in Mechanical Engineering*, 2014, 1-6.
[19] Hones, P., Zakri, C., Schmid, P.E., Lévy, F. and Shojaei, O.R., 2000. Oxidation resistance of protective coatings studied by spectroscopic ellipsometry. *Thin Solid Films*, 76, 3194-3196.
[20] Sabitzer, C., Steinkellner, C., Koller, C.M., Polcik, P., Rachbauer, R. and Mayrhofer, P.H., 2015. Diffusion behavior of C, Cr, and Fe in arc evaporated TiN- and CrN-based coatings and their influence on thermal stability and hardness. *Surface and Coatings Technology*, 275, 185-192.
[21] Otani, Y. and Hofmann, S., 1996. High temperature oxidation behaviour of ($Ti_{1-x}Cr_xN$) coatings. *Surface and Coatings Technology*, 287, 188-192.